The Influence of Additives on the Nanoscopic Dynamics of the Phospholipid Dimyristoylphosphatidylcholine

Sebastian Busch, Tobias Unruh*

Technische Universität München, Forschungsneutronenquelle Heinz Maier-Leibitz (FRM II), Lichtenbergstraße 1, 85748 Garching bei München, Germany

Physik Department E13, James-Franck-Straße 1, 85748 Garching bei München, Germany

Abstract

The influence of additives on the molecular dynamics of the phospholipid dimyristoylphosphatidylcholine (DMPC) in its fully hydrated liquid crystalline phase was studied. Quasielastic neutron scattering (QENS) was used to detect motions with dimensions of some Ångstroms on two different time scales, namely 60 ps and 900 ps. The effects of myristic acid, farnesol, cholesterol, and sodium glycocholate could consistently be explained on the basis of collective, flow-like motions of the phospholipid molecules. The influence of the additives on these motions was explained by packing effects, corresponding the reduction of free volume. Cholesterol was found to decrease the mobility of DMPC seen on the 900 ps time scale with increasing cholesterol content. In contrast, all other studied additives have no significant effect on the mobility.

Key words: DMPC, Dynamics, QENS, Myristic Acid, Farnesol, Cholesterol, Sodium Glycocholate, Dynamic Heterogeneity
PACS: 05.40.-a, 66.10.cg, 87.16.D-, 87.16.dj, 29.30.Hs

1. Introduction

The dynamics in phospholipid membranes connects to a variety of topical questions, ranging from the function of cell membranes [1] to the design of food products [2] or drug delivery systems [3, 4]. While additives are used to control the mobility accurately in the cell membrane by the organism to ensure proper functioning, they are regarded as a tool to adjust fundamental properties like storage stability and drug release in pharmaceutical technology. Due to this importance, the motions in phospholipid membranes have been studied with a variety of techniques for more than 20 years – with and without additives.

For pure phospholipids, it was found that the dynamics is much faster on a picosecond time scale as observed with quasielastic neutron scattering (QENS) than with more macroscopic techniques as e. g. fluorescence recovery after photobleaching (FRAP). This was explained with the *free volume model* [5] which states that the two techniques observe different processes. It was assumed that the fast motion which is observed by QENS corresponds to the rattling of the molecules in a cage of their neighbors from which they escape from time to time into an opening void due to thermal fluctuations. This hopping process from void to void was then thought to be the fundamental step of the slow long-range motion measured by FRAP.

To date, evidence accumulates that this microscopic picture is not correct [6, 7]. The hopping motions which were proposed as transition from the fast short-time dynamics to the slow long-time dynamics were never observed. Instead, it seems that relaxation in the membrane takes place through cooperative processes [8]. The molecules perform flow-like motions together with their neighbors, taking the cage of neighboring molecules with them [6].

These flow-like motions have so far not been detected with macroscopic techniques such as nuclear magnetic resonance (NMR), fluorescence correlation spectroscopy (FCS), or FRAP which means that the motion, i. e. the mean squared displacement (*msd*), of

*Corresponding author
Email addresses: sbusch@ph.tum.de (Sebastian Busch), tobias.unruh@frm2.tum.de (Tobias Unruh)

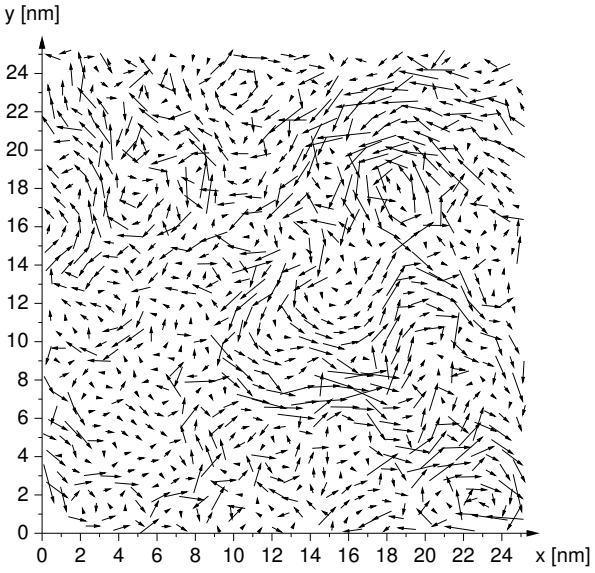

Figure 1: Visualization of flow-like motions observed in an MD simulation of a simple 2D-Lennard-Jones liquid. The arrows connect the position of the particles with a time difference of 100 ps.

a single molecule becomes diffusion-like on a submillisecond time scale. This does not conflict with a decay of the correlation between molecules on a microsecond time scale [9], which only requires that the mean-squared displacement of neighbouring molecules become diffusion-like in a correlated manner. This would for example be the case if a patch of neighboring molecules participates in several flow events in random directions: Even if the molecules in the patch itself stay correlated among each other, the trajectory of each molecule becomes diffusive.

The collective relaxations seem to be closely related to dynamic heterogeneities [10–12] observed in simple liquids, colloids, and other systems [13–19]. To demonstrate this similarity, we have performed a state-of-the art molecular dynamics (MD) simulation of a canonical (NVT) ensemble of a 2D-Lennard-Jones liquid, following previous studies [20]. The 1024 particles were distributed inside a square 2D-box of 25.237 nm side length and equilibrated for 10^6 time steps, corresponding to 1 ns, followed by a 100 ps production run. The Lennard-Jones potential between two particles i and j located at a distance r_{ij} from each other is given by

$$V_{\text{L-J}}(r_{ij}) = 4\epsilon_{ij}\left[\left(\frac{\sigma_{ij}}{r_{ij}}\right)^{12} - \left(\frac{\sigma_{ij}}{r_{ij}}\right)^{6}\right] . \qquad (1)$$

The parameter $\sigma_{ij} = 0.7\,\text{nm}$ was chosen inspired by phospholipid molecules [21, 22] and $\epsilon_{ij} = 5.0\,\text{kJ/mol}$ close to the thermal kinetic energy of particles in a two dimensional system to be in the fluid phase. Periodic boundary conditions were applied and a Berendsen temperature coupling with time constant of 50 fs to a temperature bath with 310.14 K was used.

By connecting the positions for each particle at time $t = 1.0\,\text{ns}$ with its position 100 ps later by an arrow, the picture in Fig. 1 was obtained. It can be seen that neighboring particles move often collectively with similar speeds and directions and that different areas move very differently – some patches are nearly static while others move with relatively high velocities. These are the so-called *dynamic heterogeneities*. As mentioned above, this picture strongly resembles similar representations of the simulated dynamics of DPPC molecules in bilayers [6]. The similarity of the displacement patterns observed in 2D Lennard-Jones systems and phospholipid membranes has also been observed recently in other simulations [23].

We suggest that this similarity indicates that the mobility of the molecules on the picosecond time scale is determined mainly by the closely 2D-packed head groups of the phospholipid molecules which were compared to a densely packed 2D liquid already before [22]. In comparison, the tail groups are more loosely packed at temperatures above the main phase transition [24]. From colloids, it is well known that more densely packed systems exhibit slower dynamics [25]. We assume therefore that the dense phospholipid head groups are the limiting factor for the mobility.

Independently from the validity of the microscopic mechanism, free volume is accepted to play an important role in dynamic processes – at least these quantities are positively correlated [24, 26–28]. However, we will interpret the results also in the frame of correlated, flow-like motions.

In the present article, we discuss the influence of additives on the mobility of phospholipid molecules (dimyristoylphosphatidylcholine, DMPC) in this frame. We propose that the chain-like molecules myristic acid (MA) and farnesol increase the area covered by the membrane but not the density – and do therefore not change the mobility. Cholesterol increases the density in the chain area and hereby causes a decrease of the mobility. In contrast, the co-emulsifier sodium glycocholate (NaGC, SGC) has basically no influence which can be explained by the larger hydrophilic head group.

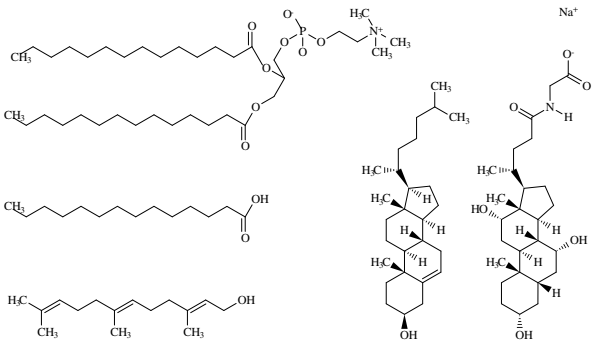

Figure 2: Structures of molecules discussed in this work. Left: Phospholipid DMPC (top), myristic acid (middle), farnesol (bottom); center: cholesterol; right: sodium glycocholate.

2. Materials and Methods

2.1. Samples

D_2O (99.90%) was supplied by Euriso-Top, Gif sur Yvette, France. The phospholipid DMPC was purchased from Lipoid GmbH, Ludwigshafen, Germany and used as received. All other substances (myristic acid, cholesterol, farnesol, and sodium glycocholate) were obtained from Sigma Aldrich, Münster, Germany and also used without further purification. The relevant molecular structures are displayed in Fig. 2.

The additives were mixed with the phospholipid in the ratios given in Table 1 with mole fractions x_{additive} of up to 40 mol%. The mixtures were then exposed to a saturated D_2O atmosphere at 40 °C for at least 48 h until a clear sample consisting of randomly-oriented liquid-crystalline domains formed. Finally, additional D_2O was added to ensure full hydration during the whole experiment. All samples were bulk samples to exclude potential disturbing effects of a support.

2.2. Basic Properties of the Samples

D_2O was used instead of H_2O because it has essentially the same chemical properties but a significantly smaller neutron scattering cross section which facilitates the subtraction of its signal.

DMPC is a typical phospholipid with amphiphilic properties due to its hydrophilic head and hydrophobic tail groups. When adding water (or D_2O), it self-assembles in bilayers and forms liquid crystalline phases. In both, H_2O and D_2O, it has a main phase transition at 24 °C which is attributed to the melting of the chains. The macroscopic diffusion coefficient below the main phase transition has been found to be about one order of magnitude below the one above the main phase transition [29]. Phospholipids like DMPC can be used

Name	[Additive]		[DMPC]
	/mol%[a]	/mass%[b]	/mass%[b]
Additive: None			
D	–	–	50.1
Additive: Myristic Acid			
M01	1.0	0.12	33.6
M02	1.7	0.20	33.5
M03	2.6	0.30	33.4
Additive: Farnesol			
F05	4.7	0.8	49.0
F09	9.1	1.6	49.0
F14	13.5	2.5	49.0
F18	17.8	3.4	48.0
Additive: Cholesterol			
C05	5.1	1.5	48.8
C10	10.0	3.0	47.1
C20	19.9	6.2	43.8
C30	30.0	9.8	40.1
C40	40.1	13.8	36.2
Additive: Sodium Glycocholate			
N05	5.2	1.7	48.5
N10	10.0	3.3	46.8
N14	13.6	3.3	32.7

Table 1: Compositions of the samples. The missing quantity up to 100% is D_2O. [a] x_{additive}, related to amount of phospholipid; [b] related to sample mass.

to stabilize dispersed particles with respect to aggregation and coalescence. In this case, DMPC acts as an interface active substance and stabilizes the particles by forming a molecular monolayer in the interface between the particle and the dispersion medium.

Myristic acid is a water-insoluble chain-like molecule which is the fatty acid contained in DMPC. Previously, it was found that stearic acid generates a slight positive excess volume at low concentrations [30]. Free fatty acids can cause cell death which was attributed to an increased membrane permeability for hydrophilic substances [31]. The phase diagram of the myristic acid - DMPC - water system as a function of the myristic acid mole fraction x_{MA} is known [32]. During the preparation of the samples, it was observed that their viscosity increased significantly with increasing amount of MA.

Farnesol is insoluble in water, too. Due to the double bonds it is stiffer than MA. It can cause apoptosis which, however, seems to be caused by interactions with proteins rather than with the membrane [33]. The phase diagram of the farnesol - DMPC - water mixture as a function of the farnesol content was studied e. g. by NMR [34, 35].

Cholesterol, also insoluble in water, is known to increase the membrane bending rigidity [36] and to suppress the phase transitions of the phospholipid [37]. Cells use it to regulate the properties of the cell membrane [38]. It is known that it has a condensing effect on the membrane, as summarized by Róg et al. [39], which corresponds to the filling-up of voids in the lipophilic core of the membrane [40]. A simultaneous decrease of phospholipid mobility was observed by several groups [24, 26, 27, 41–44] but also an increase of the dynamics has been reported [45, 46]. The motions of cholesterol in phospholipid membranes was also previously studied with QENS [47], complementary to the present study of the phospholipid motions. The phase diagram of the cholesterol - DMPC - water system is well studied, for example by differential scanning calorimetry [48] and electron paramagnetic resonance (EPR) [43].

Sodium glycocholate is a water soluble ionic surfactant with a critical micelle concentration of about 8 mM [49, 50]. It is used in the digestive system to emulsify fatty substances and hereby enabling absorption [38]. In pharmaceutical technology, it is used to stabilize dispersions which undergo a phase transition of the dispersed phase from liquid (production) to solid (storage). During crystallization, the interface of the paricles expands abruptly due to the change of the particle shape from spherical to platelet-like. In dispersions stabilized by phospholipids, it is assumed that the newly formed interface cannot be stabilized fast enough to avoid aggregation. It was found that these instabilities can be prevented when using NaGC as co-stabilizer [51]. The stabilizing property of NaGC is attributed to its high mobility. One question addressed in this contribution is whether this kind of *rapidness* in covering freshly generated interfaces can be observed by QENS. During preparation of the samples, it was observed that samples containing NaGC were more fluid and had a less turbid appearance.

2.3. Neutron Scattering

The focus of this work is the influence of additives on the motion of phospholipid molecules on a pico- to nanosecond time scale as observed with quasielastic neutron scattering. An advantage of neutron scattering with respect to other methods like electron paramagnetic resonance spectroscopy or fluorescence correlation spectroscopy is that marker molecules are not needed [52, 53].

The measurements were performed with the neutron time-of-flight spectrometer TOFTOF [54] at the research reactor FRM II (Garching, Germany), equipped with a temperature-controlled sample environment. Neutrons with well-known momentum and energy interact with the sample. The resulting changes in momentum and energy give access to structural and dynamical information, respectively [55, 56]. The uncertainty of the determination of the energy transfer between sample and neutron determines the interaction time of the neutron and the nuclei, the observation time. Several factors influence this uncertainty, among them the initial neutron wavelength and the sample geometry. Two measurement series were performed, both giving access to $Q \approx 1\,\text{Å}^{-1}$, and to time scales of 60 ps and 900 ps, respectively [57].

To realize the 60 ps measurement, the samples were filled into hollow cylindrical aluminum sample containers, minimizing self-shielding effects [58], with a sample layer thickness of 0.2 mm. An incident neutron wavelength of 6 Å, a chopper rotation speed of 12000 rpm, and a chopper ratio of 4 were chosen, leading to an elastic line width of about 60 μeV and an accessible Q range of about 0.4–1.8 Å^{-1}.

For the 900 ps measurement, a flat sample holder was used which was oriented such that its surface normal pointed to a scattering angle of 135° measured towards the location of the detectors, hereby minimizing flight-time uncertainties at the expense of a strong self-shielding around scattering angles of 45°. The corresponding spectrometer settings were 14 Å, 16000 rpm,

and ratio 8, leading to an elastic line width of only 4 μeV and an accessible Q range of about 0.1–0.8 Å^{-1}.

The raw data were converted to depend on energy transfer rather than time of flight, determining the time of flight of elastically scattered neutrons from a measurement of vanadium in the same geometry as the respective sample. All scattering intensities were corrected for self absorption effects. The energy-dependent detector efficiency was corrected and the detector sensitivities were calibrated using the elastic scattering of the vanadium standard scatterer, neglecting the smooth dependence of the scattered intensity described by the Debye-Waller factor [59].

Diffraction patterns were obtained by integrating the double differential cross section $\mathrm{d}^2\sigma/\mathrm{d}\Omega/\mathrm{d}\omega$ over an energy range $\hbar\omega$ that covered twice the instrumental resolution, similar to a so-called *elastic scan* which is often used to evaluate the motions of biomolecules.

For the evaluation of the quasielastic scattering, the double differential cross section was converted to the scattering function $S(2\theta, \omega)$ by multiplication with the ratio of the moduli of initial and final neutron wave vector [55] which was subsequently grouped into slices of constant Q [59]. For the 60 ps measurement, the bins in Q were chosen to have a distance of 0.1 Å^{-1} in the range between 0.4 and 1.8 Å^{-1} and the bins in $\hbar\omega$ ranged from -1.00 to 1.00 meV with a step width of 10 μeV. The 900 ps measurements were grouped in Q from 0.50 to 0.76 Å^{-1} in steps of 0.09 Å^{-1} and in $\hbar\omega$ from -50 to 100 μeV in steps of 1 μeV. At lower values of Q than evaluated here, the self-shielding of the flat sample geometry and the coherent scattering of the sample, cf. Fig. 3, make a reliable calculation of the incoherent scattering signal impossible. A D_2O background measurement was pro rata subtracted. The scattering angle dependent instrumental resolution was determined by the width of the elastic line of a vanadium measurement.

Due to the large incoherent neutron scattering cross section of hydrogen and the masking of the water by deuteration, the scattering signal of D_2O constitutes only about 5 % of the total scattering signal and can be subtracted without problems. The evaluated signal is caused by all organic molecules in the sample, dominated by the phospholipid due to its high concentration. Even in the samples with high cholesterol content, at least 70 % of the scattering signal are caused by the phospholipid.

2.4. Data Analysis

As done previously [7], one can create a mathematical model of the phospholipid molecules which incorporates several kinds of motion (e. g. a long-range translational flow-motion and two kinds of internal molecular reorientations). This model is fitted to the data, allowing to extract the parameter values (e. g. the width of the narrowest component which gives the flow velocity). This approach has the advantage of giving concrete numbers, for example for the flow velocity, but the disadvantage that these values can depend on the choice of model.

As this contribution is not focussed on a detailed model of molecular motion or the extraction of absolute parameter values but on the *relative change* of mobility induced by additives, a model-independent data evaluation was performed. Two quantities are suitable for that purpose: the elastically scattered intensity and the full width at half maximum. Often, the *msd* is extracted from the elastically scattered intensity. However, this method is not particularly sensitive to the long-range motion, and can easily be influenced if the background is insufficiently corrected. Therefore, the full width at half maximum (FWHM) was extracted from the scattered intensities as a function of Q. Digitization effects were avoided by a linear interpolation between the two points on either side of the half maximum [59].

To get a measure of the broadening caused by the sample on top of the instrumental resolution $\Delta(Q)$, the FWHM of the vanadium standard was subtracted from the sample FWHM to obtain $\Delta(Q)$. If the signal caused by the sample is Gaussian, $\Delta(Q)$ is indeed its FWHM. For a Lorentzian broadening, $\Delta(Q)$ is in the region of interest about 70 % of the FWHM but is in very good approximation proportional to it. It is therefore in both cases a valid measure of the broadening. All results will be shown in this form.

For the samples containing cholesterol, in an additional step we divide the $\Delta(Q)$ obtained from samples with additive by the ones of pure DMPC at the corresponding temperature. As the width is proportional to the mobility of the particles, this gives directly the ratio of mobility of the samples with additive compared to the one of pure DMPC. It was observed that the result depends hardly on Q, as expected. Therefore, an average over all values of Q was taken which we denote with *relative mobility*.

3. Results

3.1. Structural effects

The low-Q region of the diffraction patterns is shown in Fig. 3, obtained from the measurements with an incident neutron wavelength of 14 Å. It can be seen that the

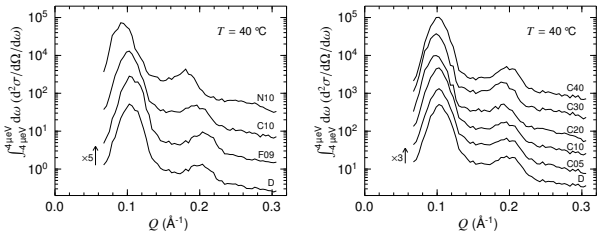

Figure 3: Diffraction patterns of selected samples, as all samples in this study fully hydrated liquid crystals at 40 °C. All diffraction patterns except the ones of pure DMPC (D) are shifted by the factors indicated in the figure. Left: influence of about 10 mol% of the additives farnesol (F), cholesterol (C), and sodium glycocholate (N) compared to pure DMPC (D). Right: changes upon increasing the cholesterol content from 0 mol% (bottom) up to 40 mol% (top).

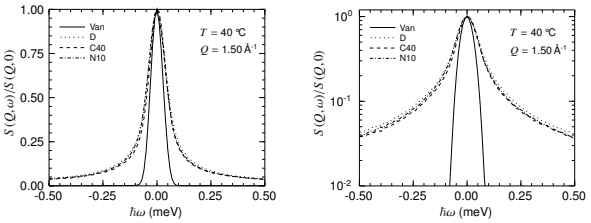

Figure 4: Plot of selected normalized spectra – pure DMPC (D), 40 mol% cholesterol (C40), and 10 mol% sodium glycocholate (N10) – measured at 40 °C shown together with the instrumental resolution as determined by a vanadium measurement (Van), as seen with an instrumental resolution of 60 μeV, corresponding to an observation time of 60 ps, at a momentum transfer of $Q = 1.5\,\text{Å}^{-1}$. The same spectra are shown on a linear scale (left) and on a logarithmic scale (right).

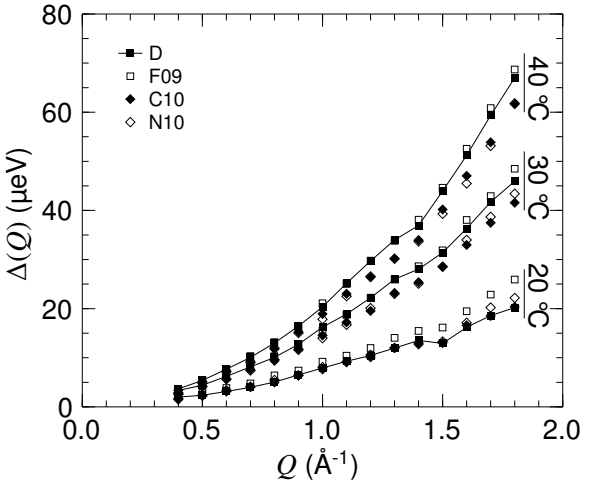

Figure 5: Broadenings (FWHM) caused by selected samples: pure DMPC (D), farnesol (F), cholesterol (C), and sodium glycocholate (N). The points of pure DMPC are connected by straight lines for better clarity. Seen with an instrumental resolution of 60 μeV, corresponding to an observation time of 60 ps, at 20 °C, 30 °C, and 40 °C.

resulting diffraction patterns drop slightly with increasing Q. This is not connected to structural properties of the sample but is rather caused by the motional broadening of the quasielastic line which makes intensity move out of the integrated energy transfer region. The peaks are caused by the coherent scattering interferences due to the repeating units of the bilayers in the direction of the surface normal.

It can be seen that the overall diffraction pattern and therefore the bilayered structure of the membrane stacks is conserved. The peak position does not shift upon addition of 10 mol% farnesol, meaning that the repeating distance of the bilayers is not affected. A shift to lower values of Q can be observed when adding either 10 mol% of cholesterol or sodium glycocholate, corresponding to an increase of the repeating distance. The trends in the diffraction patterns of cholesterol agree with the ones observed by X-ray scattering [60, 61] and MD simulations [62].

There is another correlation peak in the diffraction patterns at higher values of Q caused by the repeating distances of the chains within the membrane plane, becoming visible in the measurements using an incident neutron wavelength of 6 Å (not shown). While it is quite pronounced at $1.5\,\text{Å}^{-1}$ at 20 °C, it smears out drastically and moves to about $1.4\,\text{Å}^{-1}$ at temperatures above the chain melting transition. The additives do not change the position of this peak which does however not allow conclusions about a possible change of the area per lipid [22]. The peak height decreases with increasing cholesterol content, in agreement with previous studies [63].

3.2. Molecular mobility on a 60 ps time scale

While the diffraction patterns, obtained from integration of the energy-dependent spectra, yield information about the structure of the sample, the energy-dependence itself is connected to the motions of the molecules. Looking at a time scale of about 60 ps, the central line is visibly broadened compared to the one of a vanadium standard (instrumental resolution) of 60 μeV as can be seen in Fig. 4 exemplarily for some samples. The spectra – and therefore the observed motions – of the different samples are quite similar on this time scale.

The full width at half maximum $\Delta(Q)$ as defined above was extracted from the data at different momentum transfers Q. All spectra exhibit a line which is significantly broader than the instrumental resolution. All $\Delta(Q)$ show a small dip at $Q = 1.5\,\text{Å}^{-1}$ at 20 °C which shifts to about $1.4\,\text{Å}^{-1}$ at higher temperatures as can be

seen in Figs. 5 and 6. This is due to the so-called *de Gennes narrowing* at the structure factor maximum of a disordered phase. Therefore, these dips in $\Delta(Q)$ coincide with the peaks at large Q in the diffraction patterns discussed above.

The addition of myristic acid does not induce changes of this feature. Farnesol makes the dip less pronounced, especially at 20 °C, in contrast to cholesterol which also reduces the dip – except at 20 °C, similar to sodium glycocholate.

For a quick overview of the different effect of different substances, $\Delta(Q)$ of pure DMPC and samples with 10 mol% of all the studied additives except MA are compared with each other in Fig. 5. At 20 °C, below the main phase transition, the additives cause either no effect or an increased mobility compared to the pure DMPC. At the higher temperatures, farnesol seems to cause a small increase of the dynamics while cholesterol and NaGC slow the motions down by more or less the same amount.

Looking in more detail at the concentration dependent influence of the different additives one at a time in Fig. 6, it is evident that the addition of myristic acid has no systematic influence on the 60 ps dynamics of DMPC in its fluid phase; there is a trend towards lower mobility which is more pronounced at 20 °C. A systematic increase of the dynamics is observed for the Farnesol doped samples on the time scale of 60 ps, both, below and above the main phase transition. The addition of cholesterol does not change the dynamics at 20 °C at all but shows a clear systematic effect on the dynamics above the main phase transition. This decrease is rather continuous, compatible with NMR measurements [44]. Sodium glycocholate affects the line width similar to cholesterol above the main phase transition. Additionally, it enhances the dynamics at 20 °C slightly but not as much as farnesol.

3.3. Molecular mobility on a 900 ps time scale

On a time scale of 900 ps, the differences between the spectra are more pronounced (cf. Fig. 7). However, it becomes already clear when looking at the spectra that the influence depends very much on the type of additive: NaGC shows hardly any effect whereas cholesterol narrows the line considerably (which is still clearly broader than the instrumental resolution).

This picture is confirmed by the extracted widths $\Delta(Q)$ of the 10 mol% samples compared with the one of pure DMPC in Fig. 8: on a time scale of 900 ps and at a temperature of 40 °C, none of the probed additives causes an increase of the dynamics. Instead, farnesol and NaGC have basically no influence on the speed of the motions. Indeed, the width extracted from the samples with 10 mol% farnesol or sodium glycocholate differ by only 1% from the one of pure DMPC. In contrast, cholesterol causes a slowing down which is much more pronounced than on the 60 ps scale.

The quasielastic broadening of measurements with increasing cholesterol content is displayed in Fig. 9. The dynamics decreases continuously with increasing cholesterol concentration.

4. Discussion

Different motions dominate the *msd* of atoms and molecules and hereby the signal of a QENS experiment when studying a sample on different time scales [57]: On a short time scale, fast motions – which are mostly reorientations within the molecule – predominate. On longer time scales, these motions can only contribute a constant to the *msd* which is then governed by the slower but non-localized motions of the whole molecule. Within the short times, the molecules explore their immediate vicinity whereas the larger motions have already previously been interpreted in the frame of flow-like motions of transient assembling patches of molecules in the membrane [6, 7].

It is not surprising that these flow motions resemble the dynamical heterogeneities observed in 2D Lennard-Jones fluids, colloidal systems or granular media as the head groups form a dense 2D system. As the density in the head region is larger than the one in the tail region [24, 64], we speculate that the mobility of the phospholipid molecules in the native membranes will be governed by the interaction of the head groups.

Additives can influence the head and tail region separately by increasing or decreasing the respective density. If an additive caused a density in-/decrease in the head region, this would translate directly into a de-/increase of the DMPC mobility. For the more loosely packed tails, the connection is more intricate: A density decrease would not cause a further increase of the mobility as the head groups are the limiting factor already. Nevertheless, when increasing the density in the tail group region of a membrane by additives, a reduced mobility of DMPC molecules should be observed.

Thus, we suggest to interpret the influence of additives on the dynamics of DMPC in the liquid crystalline phase according to the amount of free volume in the DMPC bilayer created or annihilated by the intercalation of guest molecules and the influence of this free volume on the flow-like motions in the membrane. The results of our measurements, summarized in Tab. 2 for

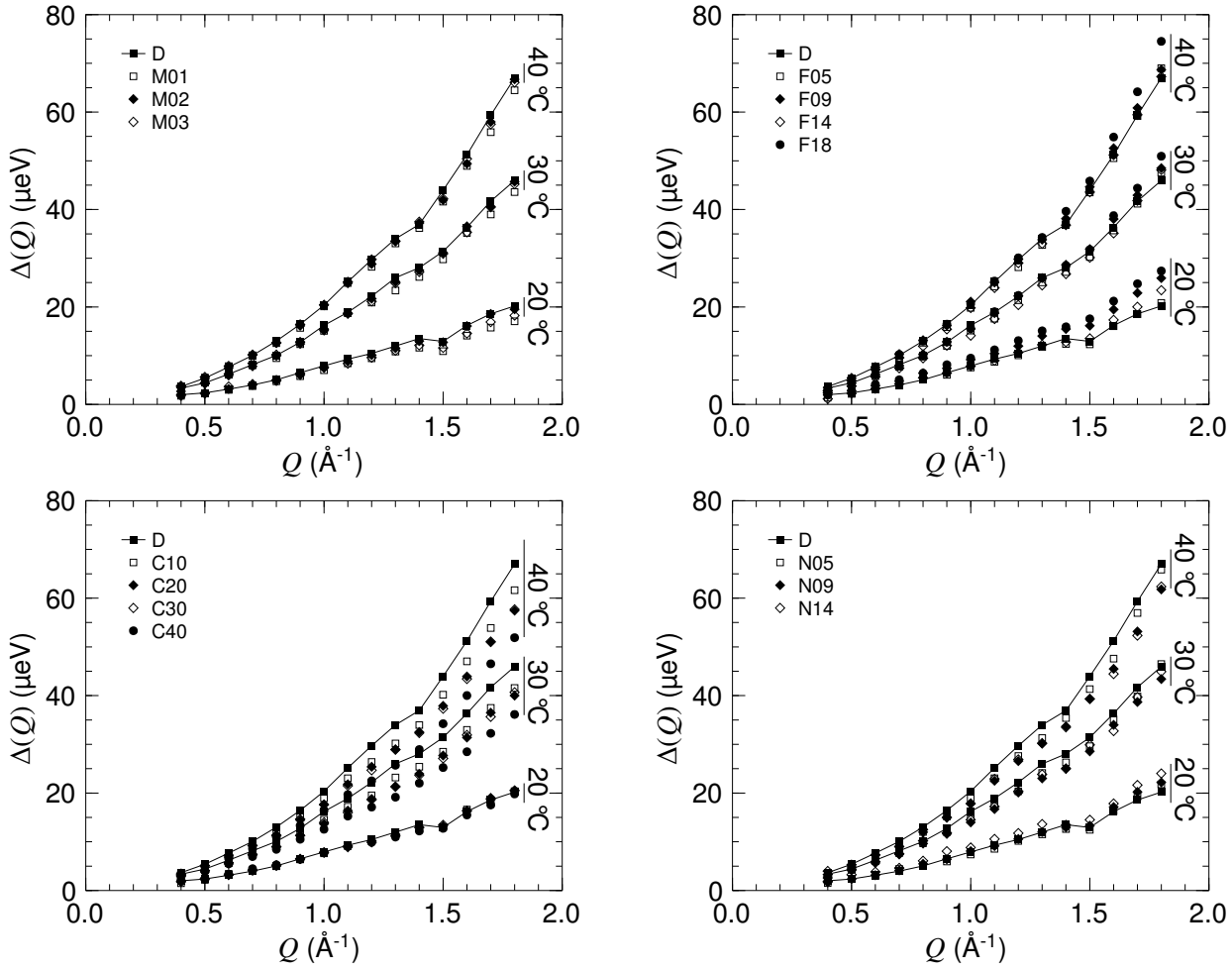

Figure 6: Broadenings (FWHM) caused by all discussed samples at all discussed temperatures as observed with an instrumental resolution of 60 μeV, corresponding to an observation time of 60 ps. Top left: myristic acid; top right: farnesol; bottom left: cholesterol; bottom right: sodium glycocholate. The points of pure DMPC are connected by straight lines for better clarity.

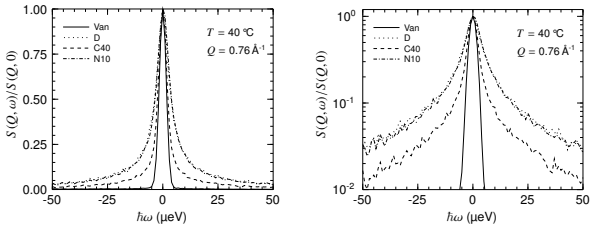

Figure 7: Plots of selected normalized spectra – pure DMPC (D), 40 mol% cholesterol (C40), and 10 mol% sodium glycocholate (N10) – measured at 40 °C shown together with the instrumental resolution as determined by a vanadium measurement (Van), as seen with an instrumental resolution of 4 μeV, corresponding to an observation time of 900 ps, at a momentum transfer of $Q = 0.76$ Å^{-1}. The same spectra are shown on a linear scale (left) and on a logarithmic scale (right).

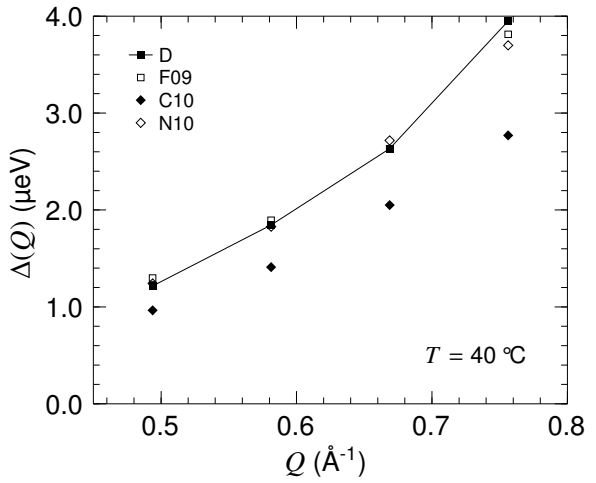

Figure 8: Broadenings (FWHM) caused by selected samples: pure DMPC (D), farnesol (F), cholesterol (C), and sodium glycocholate (N). The points of pure DMPC are connected by straight lines for better clarity. Seen with an instrumental resolution of 4 μeV, corresponding to an observation time of 900 ps, at 40 °C.

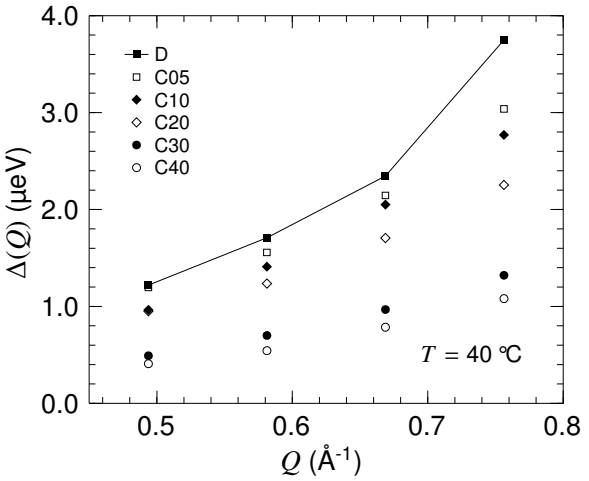

Figure 9: Broadenings (FWHM) caused by samples with increasing cholesterol content at 40 °C as observed with an instrumental resolution of 4 μeV, corresponding to an observation time of 900 ps. The points of pure DMPC are connected by straight lines for better clarity.

the different additives, are discussed in this sense below. We would like to stress that we do *not* see this as a support for the free volume theory which relies on further assumptions such as jump-like motions of the molecules.

If only the head region is densely packed, the displacements of the molecules will be caused by the density fluctuations there. If also the tail region is densely packed, the molecules will be influenced also by density fluctuations in this region. Should the fluctuations in the two regions be completely correlated, there will be no influence on the flow-like motions of the molecules. Every decorrelation between the two will decrease the persistence time of a flow event of one molecule. This interpretation also agrees with results from coarse-grained simulations which found a disrupting effect of cholesterol on the collective diffusion of the phospholipid molecules [65]. A reduction of the flow time and correspondingly flow length of a random walk translates directly in a reduction of the resulting diffusion coefficient.

4.1. Myristic Acid

Although the effects of myristic acid as an additive did not cause a significant effect on the microscopic scale (cf. Fig. 6), drastic changes of the macroscopic behavior (increasing viscosity) of the phospholipid were observed already for low myristic acid concentrations. It cannot be excluded that stronger effects would be visible if the concentration could be increased to levels comparable to, e. g., cholesterol. But this does not seem

	60 ps			900 ps
	20 °C	30 °C	40 °C	40 °C
MA	−	∅	∅	
Farnesol	++	+	+	∅
Cholesterol	∅	−−	−−	− − −
NaGC	+	−	−	∅

Table 2: Summary of the observed effects of several additives on the dynamics of DMPC on time scales of 60 and 900 ps. While ∅ indicates no change of the dynamics, the number of + and − correspond to the degree of in- or decrease of the mobility.

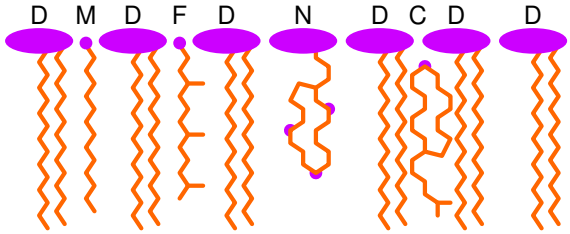

Figure 10: Sketch of the proposed configuration of the molecules, denoted by D (DMPC), M (myristic acid), F (farnesol), N (NaGC), and C (cholesterol). The hydrophilic parts are schematically displayed as violet bubbles, the hydrophobic chains and steroid as orange sticks.

not to be very likely because myristic acid is a chain-like molecule and can thus be expected to be oriented mainly parallel to the DMPC chains. The hydrophilic carboxyl group can be expected to stick into the head-group region of the DMPC layers. Therefore, myristic acid should not fill up free volume in the tail region of DMPC bilayers and should also not alter their head group packing significantly [30]. This is in agreement with corresponding studies using short chain alcohols as additives where also no effect on the phospholipid dynamics was observed [66].

4.2. Farnesol

The behavior of farnesol inside DMPC bilayers seems to be similar to the one of myristic acid. From NMR measurements, it could not be determined whether the molecules intercalate between the DMPC molecules or are placed in between the two leaflets [35]. The diffraction patterns in Fig. 3 show no influence of Farnesol on peak distance and height of the first two layer repeating peaks. Although we cannot exclude that a change in the bilayer thickness is exactly componsated by an accompanying change in water thickness, we see no evidence for a change of the bilayer thickness upon the addition of farnesol. This indicates that the molecules intercalate between the DMPC molecules. Respecting that the effect on the mobility of DMPC is negligible, we conclude that the molecules align themselves along the phospholipid molecules similar to the case of myristic acid. It is known from NMR measurements [34] that farnesol has a different influence on the surrounding phospholipid molecules compared to cholesterol. While cholesterol causes an increase of the molecular oder parameters, farnesol does not. However, farnesol lowers the main phase transition temperature which might explain the unusual increased dynamics at 20 °C: the addition of farnesol probably induces a melting of the phospholipid chains.

4.3. Cholesterol

Cholesterol causes an increasing thickness of the membrane. This was also observed by X-ray diffraction and simulations and reflects the condensation effect [39, 60, 61]. The incorporation of cholesterol into the phospholipid membrane can be understood in the frame of the umbrella model [67]: The hydrophobic cholesterol molecule resides between the hydrophobic tails of the phospholipids. The hydrophilic heads of the phospholipid shield the tails and cholesterol from the surrounding water. This leads to an increase of the density in the hydrophobic part of the bilayers.

This density increase reduces the free volume in the chain region of the DMPC molecules. In this situation, the mobility of the phospholipid molecules is no more mainly determined by the dynamic inhomogeneities in the densely packed head groups but also by those in the now more closely packed tail groups resulting in a significantly slower molecular transport.

The influence of cholesterol on DMPC as seen with quasielastic neutron scattering in the present study is summarized in Fig. 11: the widths $\Delta(Q)$ are normalized to the widths of pure DMPC at the same temperature and averaged over all Q values, yielding the *relative mobility*. It can immediately be seen that in no case addition of cholesterol causes an increased dynamics of DMPC.

The motions detected within an observation time of 60 ps are not affected by the addition of cholesterol at temperatures below the main phase transition. At temperatures above the main phase transition, the tails experience the density increase caused by cholesterol. The relative decrease of the linewidth is completely identical at 30 °C and 40 °C for all measured cholesterol concentrations which indicates that the observed motions are not sensitive to the absolute distance from the phase transition temperature as one might expect for local motions.

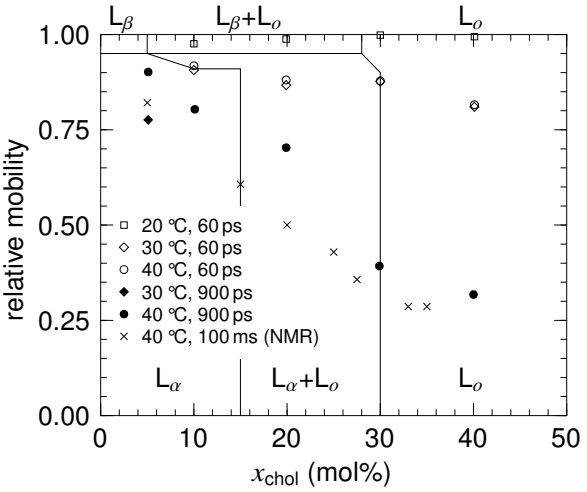

Figure 11: The relative mobility (mobility normalized to the one of pure DMPC, cf. text) as a function of cholesterol concentration at different temperatures. Open symbols are extracted from measurements with an instrumental resolution of 60 μeV, corresponding to an observation time of 60 ps; closed symbols are extracted from measurements with an instrumental resolution of 4 μeV, corresponding to an observation time of 900 ps. NMR measurements taken from Filippov et al. [44] at 40 °C are also shown. The phase boundaries are drawn after EPR results of Sankaram [43] and are only valid for the displayed measurements. They are only displayed to show the respective phases of the measurements and do not represent a phase diagram.

The mobility decrease of DMPC is enhanced when looking on a time scale of 900 ps where the influence of 5 mol% cholesterol affects the phospholipids more strongly at 30 °C than at 40 °C. The corresponding motions are, therefore, more sensitive to an increase in density if the sample temperature is closer to the main phase transition temperature which we see again as a signature of the long-range nature of this motion.

Also other techniques were used to measure the long-range motion of the phospholipid molecules. MD simulations [24] of the phospholipid DPPC at 50 °C, i. e. 8 K above the main phase transition of pure DPPC, show a strong impact of cholesterol on the phospholipid mobility on a 100 ns time scale – stronger than our measurements at 40 °C, even a bit more than the one at 30 °C, i. e. 6 K above the main phase transition of pure DMPC.

Fluorescence correlation spectroscopy of the phospholipid DLPC [42] on a 10 ms time scale at 25 °C, i. e. 27 K above the main phase transition of DLPC, shows an impact of cholesterol on the dynamics which is very comparable to the results obtained on a 100 ms time scale with NMR [44] for DMPC at 40 °C.

The comparison between all these results is not straightforward as different temperatures and even phospholipids were used. Only the NMR measurements were done with exactly same temperature and phospholipid as studied here and show a very good agreement with our results. All these techniques measure on longer time scales than QENS and we would therefore expect them to show a stronger impact on the dynamics – as they do. The NMR data also show a stronger influence of cholesterol on the phospholipid motions the closer the temperature to the main phase transition is.

Much in contrast, two measurements on even larger time (about 10 s) and length scales using FRAP [41, 43] observed a smaller impact of cholesterol on the dynamics. The degree varies between the measurements, one [43] even observes no impact up to about 15 mol% cholesterol in the sample. The difference between the FRAP measurements and the values obtained by NMR were discussed in terms of the susceptibility of FRAP to the formation of microdomains in the membrane [44].

4.4. Sodium glycocholate

Sodium glycocholate is a charged molecule. It is known that charged phospholipids induce an increase of the thickness of the water layer between the bilayers but not of the membrane itself [68]. This swelling is the thickness increase observed in the diffraction patterns. At low concentrations, the influence of NaGC on the dynamics of the phospholipid is similar to the one of cholesterol. However, cholesterol is uncharged, has not such an influence on the structure and can, therefore, be present in membranes in much higher concentrations.

The practical importance of sodium glycocholate is based on its ability to stabilize emulsions even during crystallization of the oily phase. In the case of triglyceride or alkane nanoemulsions, the shape of the stabilized particles changes drastically during crystallization: from a spherical droplet to an elongated crystalline platelet. This is connected to a sudden increase of the surface of the particle. One could imagine that this results in a partial coverage of the particle with stabilizer – the uncovered surfaces are then the origin of aggregation. A redistribution of the stabilizer onto the naked surface could prevent aggregation, happens however so slowly that the aggregation took place before.

As the addition of sodium glycocholate prevents aggregation, it could have had the effect of enhancing the dynamics of the phospholipid, making the redistribution of the stabilizer so fast that aggregation is suppressed.

However, sodium glycocholate does not influence the phospholipid dynamics. It can be excluded that it did not mix with the phospholipid because it is water soluble, caused a decrease of viscosity, made the sample more transparent, and changed the bilayer spacing. As NaGC is hydrophilic, an enhanced partition

into the chain region should not be expected. We see two likely structural arrangements: Either the NaGC is intercalated inside the bilayer oriented with the hydrophilic part in the region of the phospholipid head groups and the hydrophobic part in the chain region of the bilayer. Obviously, this leads to hardly any change in the free volume in either region of the membrane. Or – as already previously speculated for sodium cholate in lecithin [69] – a flat placement of the molecules on the bilayer in the head region. This would lead to a density decrease in the tail region which would, as we have argued before, not influence the dynamics.

4.5. Other influences on membrane dynamics

Using NMR, the influence of the antimicrobial peptide gramicidin was found to be comparable to the one of cholesterol on a sub-nanosecond time scale [70]. Also neutron scattering experiments showed a decreased mobility on a time scale of about 150 ps [71]. Our results are in good agreement with the view that the effects caused by gramicidin are directly comparable with the ones caused by cholesterol. However, we would like to point out that the underlying mechanism might be very different as gramicidin is approximatively barrel-like [72] and does therefore not increase the density in the tail region. However, the same study showed that the hydration of the phospholipid molecules in the vicinity of the peptide is decreased. A decreased hydration is in turn known to decrease the dynamics [73] so the decreased hydration might actually influence the dynamics more than the change in density.

In MD simulations, it was observed that proteins in the membrane cause a slowing down of adjacent phospholipid molecules [23]. This effect could be reproduced for a number of different proteins in the membrane and also 2D Lennard-Jones systems which suggests that this effect is partly caused by the obstacles hindering phospholipid motions, and complemented by specific effects due to protein-lipid interactions.

Whereas these interactions of phospholipids with peptides and proteins might be dominated by other effects than density changes, their aforementioned use as stabilizer in suspensions and emulsions could be directly influenced by the density as it might very well be that the amount of phospholipid is lower than what one would need for a full monolayer around the particles. Preliminary results indeed seem to show that the effect of decreasing mobility upon increasing density can hereby be reversed, observing increasing dynamics when artificially decreasing the density by stretching a monolayer [28, 74].

5. Conclusion

Summarizing, we studied the effect of several additives on the dynamics of the phospholipid DMPC on time scales of 60 ps and 900 ps. Myristic acid and farnesol, two more linear, chain-like molecules seem to incorporate into the membrane without modification of the mobility. Cholesterol has a pronounced slowing down effect on the dynamics. This effect can be qualitatively understood assuming that the persistence lengths of flow patterns decrease. The flow-like mobility of the molecules are the equivalent to dynamic heterogeneities observed in supercooled liquids, suspensions and granular systems. Sodium glycocholate has – in contrast to its strong macroscopic influences – no effect on the mobility.

6. Acknowledgement

We would like to thank W. Petry for his enduring interest and support as well as L. C. Pardo, T. Gutberlet, and J. Horbach for many stimulating discussions.

References

[1] D. Axelrod, Lateral motion of membrane proteins and biological function, The Journal of Membrane Biology 75 (1) (1983) 1, doi:10.1007/bf01870794.

[2] L. Sagalowicz, M. E. Leser, Delivery systems for liquid food products, Current Opinion in Colloid & Interface Science 15 (1-2) (2010) 61, doi:10.1016/j.cocis.2009.12.003.

[3] C. Peetla, A. Stine, V. Labhasetwar, Biophysical Interactions with Model Lipid Membranes: Applications in Drug Discovery and Drug Delivery., Mol. Pharm. 6 (5) (2009) 1264–76, doi:10.1021/mp9000662.

[4] K. Kawano, E. Onose, Y. Hattori, Y. Maitani, Higher liposomal membrane fluidity enhances the in vitro antitumor activity of folate-targeted liposomal mitoxantrone., Mol. Pharm. 6 (1) (2009) 98–104, doi:10.1021/mp800069c.

[5] W. L. C. Vaz, P. F. F. Almeida, Microscopic versus macroscopic diffusion in one-component fluid phase lipid bilayer-membranes, Biophys. J. 60 (6) (1991) 1553–1554, ISSN 0006-3495.

[6] E. Falck, T. Róg, M. Karttunen, I. Vattulainen, Lateral diffusion in lipid membranes through collective flows., J. Am. Chem. Soc. 130 (1) (2008) 44–5, doi:10.1021/ja7103558.

[7] S. Busch, C. Smuda, L. C. Pardo, T. Unruh, Molecular Mechanism of Long-Range Diffusion in Phospholipid Membranes Studied by Quasielastic Neutron Scattering, Journal of the American Chemical Society 132 (10) (2010) 3232, doi:10.1021/ja907581s.

[8] M. C. Rheinstädter, J. Das, E. Flenner, B. Brüning, T. Seydel, I. Kosztin, Motional Coherence in Fluid Phospholipid Membranes, Physical Review Letters 101 (24) (2008) 248106, doi:10.1103/physrevlett.101.248106.

[9] T. Apajalahti, P. S. Niemelä, P. N. Govindan, M. S. Miettinen, E. Salonen, S.-J. Marrink, I. Vattulainen, Concerted diffusion of lipids in raft-like membranes, Faraday Discussions 144 (2010) 411, doi:10.1039/b901487j.

[10] W. Kob, C. Donati, S. Plimpton, P. Poole, S. C. Glotzer, Dynamical Heterogeneities in a Supercooled Lennard-Jones Liquid, Physical Review Letters 79 (15) (1997) 2827, doi: 10.1103/physrevlett.79.2827.

[11] C. Donati, J. Douglas, W. Kob, S. Plimpton, P. Poole, S. C. Glotzer, Stringlike Cooperative Motion in a Supercooled Liquid, Physical Review Letters 80 (11) (1998) 2338, doi: 10.1103/physrevlett.80.2338.

[12] H. R. Schober, C. Gaukel, C. Oligschleger, Collective Jumps in Amorphous Materials, Defect and Diffusion Forum 143-147 (1997) 723, doi:10.4028/www.scientific.net/ddf.143-147.723.

[13] R. Richert, Heterogeneous dynamics in liquids: fluctuations in space and time, Journal of Physics: Condensed Matter 14 (23) (2002) R703, doi:10.1088/0953-8984/14/23/201.

[14] A. Marcus, J. Schofield, S. A. Rice, Experimental observations of non-Gaussian behavior and stringlike cooperative dynamics in concentrated quasi-two-dimensional colloidal liquids, Physical Review E 60 (5) (1999) 5725, doi: 10.1103/physreve.60.5725.

[15] W. K. Kegel, Direct Observation of Dynamical Heterogeneities in Colloidal Hard-Sphere Suspensions, Science 287 (5451) (2000) 290, doi:10.1126/science.287.5451.290.

[16] B. Cui, B. Lin, S. A. Rice, Dynamical heterogeneity in a dense quasi-two-dimensional colloidal liquid, The Journal of Chemical Physics 114 (20) (2001) 9142, doi:10.1063/1.1369129.

[17] R. Zangi, S. A. Rice, Cooperative Dynamics in Two Dimensions, Physical Review Letters 92 (3) (2004) 035502, doi: 10.1103/physrevlett.92.035502.

[18] A. S. Keys, A. R. Abate, S. C. Glotzer, D. J. Durian, Measurement of growing dynamical length scales and prediction of the jamming transition in a granular material, Nature Physics 3 (4) (2007) 260, doi:10.1038/nphys572.

[19] R. Matena, M. Dijkstra, A. Patti, Non-Gaussian dynamics in smectic liquid crystals of parallel hard rods, Physical Review E 81 (2) (2010) 021704, doi:10.1103/physreve.81.021704.

[20] M. Hurley, P. Harrowell, Kinetic structure of a two-dimensional liquid, Physical Review E 52 (2) (1995) 1694, doi: 10.1103/physreve.52.1694.

[21] S. Tristram-Nagle, Y. Liu, J. Legleiter, J. F. Nagle, Structure of Gel Phase DMPC Determined by X-Ray Diffraction, Biophysical Journal 83 (6) (2002) 3324, doi:10.1016/s0006-3495(02)75333-2.

[22] J. S. Hub, T. Salditt, M. C. Rheinstädter, B. L. de Groot, Short-range order and collective dynamics of DMPC bilayers: a comparison between molecular dynamics simulations, X-ray, and neutron scattering experiments., Biophys. J. 93 (9) (2007) 3156–68, doi:10.1529/biophysj.107.104885.

[23] P. S. Niemelä, M. S. Miettinen, L. Monticelli, H. Hammaren, P. Bjelkmar, T. Murtola, E. Lindahl, I. Vattulainen, Membrane Proteins Diffuse as Dynamic Complexes with Lipids, Journal of the American Chemical Society (2010) 100514104303095doi: 10.1021/ja101481b.

[24] E. Falck, M. Patra, M. Karttunen, M. T. Hyvönen, I. Vattulainen, Lessons of slicing membranes: interplay of packing, free area, and lateral diffusion in phospholipid/cholesterol bilayers., in: [26] (2004) 1076–91, doi:10.1529/biophysj.104.041368.

[25] P. N. Pusey, W. van Megen, Observation of a glass transition in suspensions of spherical colloidal particles, Physical Review Letters 59 (18) (1987) 2083, doi:10.1103/physrevlett.59.2083.

[26] P. F. F. Almeida, W. L. C. Vaz, T. E. Thompson, Lipid diffusion, free area, and molecular dynamics simulations., in: [27] (2005) 4434–8, doi:10.1529/biophysj.105.059766.

[27] E. Falck, M. Patra, M. Karttunen, M. T. Hyvönen, I. Vattulainen, Response to comment by Almeida et al.: free area theories for lipid bilayers–predictive or not?, Biophys. J. 89 (1) (2005) 745–52, doi:10.1529/biophysj.105.065714.

[28] M. Javanainen, L. Monticelli, J. B. de la Serna, I. Vattulainen, Free Volume Theory Applied to Lateral Diffusion in Langmuir Monolayers: Atomistic Simulations for a Protein-Free Model of Lung Surfactant, Langmuir (2010) in pressdoi: 10.1021/la102454m.

[29] S. Ghosh, A. Adhikari, S. Sen Mojumdar, K. Bhattacharyya, A Fluorescence Correlation Spectroscopy Study of the Diffusion of an Organic Dye in the Gel Phase and Fluid Phase of a Single Lipid Vesicle., The journal of physical chemistry. B 114 (17) (2010) 5736–41, doi:10.1021/jp911971p.

[30] G. Peters, F. Hansen, M. Møller, P. Westh, Effects of Fatty Acid Inclusion in a DMPC Bilayer Membrane., The journal of physical chemistry B 113 (1) (2009) 92–102, doi: 10.1021/jp806205m.

[31] V. Oberle, Untersuchungen zum Einfluß freier Fettsäuren auf die Eigenschaften biologischer und Modellmembranen, Ph.D. thesis, Martin-Luther-Universität, Halle (Saale), 1999.

[32] R. Koynova, B. Tenchov, G. Rapp, Mixing behavior of saturated short-chain phosphatidylcholines and fatty acids Eutectic points, liquid and solid phase immiscibility, non-lamellar phases, Chemistry and Physics of Lipids 88 (1) (1997) 45, doi: 10.1016/s0009-3084(97)00043-1.

[33] J. Joo, A. Jetten, Molecular mechanisms involved in farnesol-induced apoptosis., Cancer Lett. 287 (2) (2010) 123–35, doi: 10.1016/j.canlet.2009.05.015.

[34] A. C. Rowat, J. H. Davis, Farnesol-DMPC phase behaviour: a (2)H-NMR study., Biochim. Biophys. Acta 1661 (2) (2004) 178–87, doi:10.1016/j.bbamem.2004.01.002.

[35] A. C. Rowat, D. Keller, J. H. Ipsen, Effects of farnesol on the physical properties of DMPC membranes., Biochim. Biophys. Acta 1713 (1) (2005) 29–39, doi: 10.1016/j.bbamem.2005.04.014.

[36] G. Orädd, V. Shahedi, G. Lindblom, Effect of sterol structure on the bending rigidity of lipid membranes: A 2H NMR transverse relaxation study, Biochimica et Biophysica Acta (BBA) - Biomembranes 1788 (9) (2009) 1762–71, doi: 10.1016/j.bbamem.2009.06.019.

[37] D. A. Mannock, R. N. Lewis, R. N. McElhaney, A Calorimetric and Spectroscopic Comparison of the Effects of Ergosterol and Cholesterol on the Thermotropic Phase Behavior and Organization of Dipalmitoylphosphatidylcholine Bilayer Membranes., Biochim. Biophys. Acta 1798 (3) (2010) 376–88, doi: 10.1016/j.bbamem.2009.09.002.

[38] J. M. Berg, J. L. Tymoczko, L. Stryer, Biochemie., Spektrum Akademischer Verlag, 5. a. edn., ISBN 9783827413031, 2003.

[39] T. Róg, M. Pasenkiewicz-Gierula, I. Vattulainen, M. Karttunen, Ordering effects of cholesterol and its analogues., Biochim. Biophys. Acta 1788 (1) (2009) 97–121, doi: 10.1016/j.bbamem.2008.08.022.

[40] E. Falck, M. Patra, M. Karttunen, M. T. Hyvönen, I. Vattulainen, Impact of cholesterol on voids in phospholipid membranes., The Journal of chemical physics 121 (24) (2004) 12676–89, doi: 10.1063/1.1824033.

[41] J. L. Rubenstein, B. A. Smith, H. M. McConnell, Lateral diffusion in binary mixtures of cholesterol and phosphatidylcholines., Proc. Natl. Acad. Sci. U.S.A. 76 (1) (1979) 15–8.

[42] J. Korlach, P. Schwille, W. W. Webb, G. W. Feigenson, Characterization of lipid bilayer phases by confocal microscopy and fluorescence correlation spectroscopy., Proc. Natl. Acad. Sci. U.S.A. 96 (15) (1999) 8461–6.

[43] P. F. F. Almeida, W. L. C. Vaz, T. E. Thompson, Lateral diffusion in the liquid phases of dimyristoylphosphatidylcholine/cholesterol lipid bilayers: a free volume analysis, Biochemistry 31 (29) (1992) 6739, doi:10.1021/bi00144a013.

[44] A. Filippov, G. Orädd, G. Lindblom, The Effect of Cholesterol on the Lateral Diffusion of Phospholipids in Oriented Bilayers, Biophysical Journal 84 (5) (2003) 3079, doi:10.1016/s0006-3495(03)70033-2.

[45] A.-L. Kuo, C. G. Wade, Lipid lateral diffusion by pulsed nuclear magnetic resonance, Biochemistry 18 (11) (1979) 2300, doi:10.1021/bi00578a026.

[46] J. Zidar, F. Merzel, M. Hodošček, K. Rebolj, K. Sepčić, P. Maček, D. Janežič, Liquid-Ordered Phase Formation in Cholesterol/Sphingomyelin Bilayers: All-Atom Molecular Dynamics Simulations, The Journal of Physical Chemistry B 113 (2009) 15795, doi:10.1021/jp907138h.

[47] C. Gliss, O. Randel, H. Casalta, E. Sackmann, R. Zorn, T. M. Bayerl, Anisotropic Motion of Cholesterol in Oriented DPPC Bilayers Studied by Quasielastic Neutron Scattering: The Liquid-Ordered Phase, Biophysical Journal 77 (1) (1999) 331, doi:10.1016/s0006-3495(99)76893-1.

[48] R. Tampe, A. Von Lukas, H.-J. Galla, Glycophorin-induced cholesterol-phospholipid domains in dimyristoylphosphatidylcholine bilayer vesicles, Biochemistry 30 (20) (1991) 4909, doi:10.1021/bi00234a011.

[49] P. Schurtenberger, N. Mazer, W. Känzig, Micelle to vesicle transition in aqueous solutions of bile salt and lecithin, The Journal of Physical Chemistry 89 (6) (1985) 1042, doi:10.1021/j100252a031.

[50] K. Matsuoka, M. Maeda, Y. Moro, Micelle formation of sodium glyco- and taurocholates and sodium glyco- and taurodeoxycholates and solubilization of cholesterol into their micelles, Colloids and Surfaces B: Biointerfaces 32 (2) (2003) 87, doi:10.1016/s0927-7765(03)00148-6.

[51] K. Westesen, B. Siekmann, Investigation of the gel formation of phospholipid-stabilized solid lipid nanoparticles, International Journal of Pharmaceutics 151 (1) (1997) 35, doi:10.1016/s0378-5173(97)04890-4.

[52] S. Teixeira, J. Ankner, M.-C. Bellissent-Funel, R. Bewley, M. Blakeley, L. Coates, R. Dahint, R. Dalgliesh, N. Dencher, J. Dhont, P. Fischer, V. Forsyth, G. Fragneto, B. Frick, T. Geue, R. Gilles, T. Gutberlet, M. Haertlein, T. Hauß, W. Häußler, W. Heller, K. Herwig, O. Holderer, F. Jurányi, R. Kampmann, R. Knott, J. Kohlbrecher, S. Kreuger, P. Langan, R. E. Lechner, G. Lynn, C. Majkrzak, R. May, F. Meilleur, Y. Mo, K. Mortensen, D. Myles, F. Natali, C. Neylon, N. Niimura, J. Ollivier, A. Ostermann, J. Peters, J. Pieper, A. Rühm, D. Schwahn, K. Shibata, A. Soper, T. Strässle, U. Suzuki, I. Tanaka, M. Tehei, P. Timmins, N. Torikai, T. Unruh, V. Urban, R. Vavrin, K. Weiss, G. Zaccai, New sources and instrumentation for neutrons in biology., Chemical Physics 345 (2-3) (2008) 133–151, doi:10.1016/j.chemphys.2008.02.030.

[53] V. García Sakai, A. Arbe, Quasielastic neutron scattering in soft matter, Current Opinion in Colloid & Interface Science 14 (6) (2009) 381, doi:10.1016/j.cocis.2009.04.002.

[54] T. Unruh, J. Neuhaus, W. Petry, The high-resolution time-of-flight spectrometer TOFTOF, in: [75] (2007) 1414–1422, ISSN 0168-9002, doi:10.1016/j.nima.2007.07.015.

[55] A. Furrer, J. Mesot, T. Strässle, Neutron Scattering in Condensed Matter Physics (Neutron Techniques and Applications) (Series on Neutron Techniques and Applications), World Scientific Publishing Company, 1 edn., ISBN 9789810248314, 2009.

[56] M. Bée, Quasielastic Neutron Scattering, Taylor & Francis, ISBN 9780852743713, 1988.

[57] T. Unruh, C. Smuda, S. Busch, J. Neuhaus, W. Petry, Diffusive motions in liquid medium-chain n-alkanes as seen by quasielastic time-of-flight neutron spectroscopy, The Journal of Chemical Physics 129 (2008) 121106, doi:10.1063/1.2990026.

[58] J. Wuttke, Improved sample holder for multidetector neutron spectrometers, Physica B Condensed Matter 266 (1-2) (1999) 112, doi:10.1016/s0921-4526(98)01503-8.

[59] J. Wuttke, Frida1: Fast Reliable Interactive Data Analysis, `http://sourceforge.net/projects/frida/`, URL `http://sourceforge.net/projects/frida/`, software, 1990–.

[60] W.-C. Hung, M.-T. Lee, F.-Y. Chen, H. W. Huang, The condensing effect of cholesterol in lipid bilayers., Biophys. J. 92 (11) (2007) 3960–7, doi:10.1529/biophysj.106.099234.

[61] B. Brüning, M. C. Rheinstädter, A. Hiess, B. Weinhausen, T. Reusch, S. Aeffner, T. Salditt, Influence of cholesterol on the collective dynamics of the phospholipid acyl chains in model membranes., The European physical journal. E, Soft matter doi:10.1140/epje/i2010-10574-6.

[62] M. Alwarawrah, J. Dai, J. Huang, A Molecular View of the Cholesterol Condensing Effect in DOPC Lipid Bilayers, The Journal of Physical Chemistry B 114 (22) (2010) 7516–23, doi:10.1021/jp101415g.

[63] S. W. Hui, N. B. He, Molecular organization in cholesterol-lecithin bilayers by x-ray and electron diffraction measurements, Biochemistry 22 (5) (1983) 1159, doi:10.1021/bi00274a026.

[64] S. J. Marrink, R. M. Sok, H. J. C. Berendsen, Free volume properties of a simulated lipid membrane, The Journal of Chemical Physics 104 (22) (1996) 9090, doi:10.1063/1.471442.

[65] G. S. Ayton, G. A. Voth, Mesoscopic lateral diffusion in lipid bilayers., Biophys. J. 87 (5) (2004) 3299–311, doi:10.1529/biophysj.104.047811.

[66] T. Gutberlet, D. Posselt, T. Unruh, Influence of short chain alcohols on local dynamics of DMPC, Experimental Report 935, Forschungsneutronenquelle Heinz Maier-Leibnitz (FRM II), Technische Universität München, Germany, 2008.

[67] J. Huang, A Microscopic Interaction Model of Maximum Solubility of Cholesterol in Lipid Bilayers, Biophysical Journal 76 (4) (1999) 2142, doi:10.1016/s0006-3495(99)77369-8.

[68] R. P. Rand, Interacting phospholipid bilayers: measured forces and induced structural changes., Annu. Rev. Biophys. Bioeng. 10 (1981) 277–314, doi:10.1146/annurev.bb.10.060181.001425.

[69] J. Ulmius, G. Lindblom, H. Wennerstroem, L. B. A. Johansson, K. Fontell, O. Soederman, G. Arvidson, Molecular organization in the liquid-crystalline phases of lecithin-sodium cholate-water systems studied by nuclear magnetic resonance, Biochemistry 21 (7) (1982) 1553, doi:10.1021/bi00536a014.

[70] Z. Y. Peng, V. Simplaceanu, S. R. Dowd, C. Ho, Effects of cholesterol or gramicidin on slow and fast motions of phospholipids in oriented bilayers., Proc. Natl. Acad. Sci. U.S.A. 86 (22) (1989) 8758–62.

[71] U. Wanderlingh, G. D'Angelo, V. Conti Nibali, M. Gonzalez, C. Crupi, C. Mondelli, Influence of gramicidin on the dynamics of DMPC studied by incoherent elastic neutron scattering, Journal of Physics Condensed Matter 20 (10) (2008) 104214, doi:10.1088/0953-8984/20/10/104214.

[72] J. A. Killian, B. De Kruijff, Importance of hydration for gramicidin-induced hexagonal HII phase formation in dioleoylphosphatidylcholine model membranes, Biochemistry 24 (27) (1985) 7890, doi:10.1021/bi00348a007.

[73] S. König, W. Pfeiffer, T. M. Bayerl, D. Richter, E. Sackmann, Molecular dynamics of lipid bilayers studied by incoherent quasi-elastic neutron scattering, Journal de Physique II France 2 (8) (1992) 1589, doi:10.1051/jp2:1992100.

[74] S. Busch, et al., in preparation .

[75] T. Unruh, J. Neuhaus, W. Petry, The high-resolution time-of-flight spectrometer TOFTOF (vol 580, pg 1414, 2007), Nucl. Instrum. Methods Phys. Res., Sect. A 585 (3) (2008) 201, ISSN 0168-9002, doi:10.1016/j.nima.2007.11.019.